Quantum lifetime in ultrahigh quality GaAs quantum wells: Relationship to Δ_{5/2} and impact of density fluctuations

Q. Qian, J. Nakamura, S. Fallahi, G. C. Gardner, J. D. Watson, S. Lüscher, J. A. Folk, G. A. Csáthy, and M. J. Manfra

Phys. Rev. B **96**, 035309 — Published 25 July 2017

DOI: 10.1103/PhysRevB.96.035309

Quantum Lifetime in Ultra-High Quality GaAs Quantum Wells: Relationship to $\Delta_{5/2}$ and Impact of Density Fluctuations

Q. Qian,[1,2] J. Nakamura,[1,2] S. Fallahi,[1,2,3] G. C. Gardner,[2,3,4] J. D. Watson,[1,3] S. Lüscher,[5,6] J. A. Folk,[5,6] G. A. Csáthy,[1] and M. J. Manfra[1,2,3,4,7,*]

[1]*Department of Physics and Astronomy, Purdue University, West Lafayette, Indiana 47907, USA*

[2]*Station Q Purdue, Purdue University, West Lafayette, Indiana 47907, USA*

[3]*Birck Nanotechnology Center, Purdue University, West Lafayette, Indiana 47907, USA*

[4]*School of Materials Engineering, Purdue University, West Lafayette, Indiana 47907, USA*

[5]*Department of Physics and Astronomy, University of British Columbia, Vancouver, BC V6T 1Z1, Canada*

[6]*Quantum Matter Institute, University of British Columbia, Vancouver, BC V6T 1Z4, Canada*

[7]*School of Electrical and Computer Engineering, Purdue University, West Lafayette, Indiana 47907, USA*

Abstract

We consider quantum lifetime derived from low-field Shubnikov-de Haas oscillations as a metric of quality of the two-dimensional electron gas in GaAs quantum wells that expresses large excitation gaps of the $\nu = \frac{5}{2}$ fractional quantum Hall state in the N=1 Landau level. In high quality samples small density inhomogeneities dramatically impact the amplitude of Shubnikov-de Haas oscillations such that the canonical method (cf. Coleridge, Phys. Rev. B **44**, 3793) for determination of quantum lifetime substantially underestimates $\tau_{\rm q}$ unless density inhomogeneity is explicitly considered. We have developed a method which can be used to determine density inhomogeneity and extract the intrinsic $\tau_{\rm q}$ by analyzing the Shubnikov-de Haas oscillations. However, even after accounting for inhomogeneity, $\tau_{\rm q}$ does not correlate well with sample quality as measured by $\Delta_{5/2}$, the excitation gap of the fractional quantum Hall state at 5/2 filling.

I. INTRODUCTION

Improvements in heterostructure design and molecular beam epitaxy (MBE) techniques have made it possible to grow AlGaAs/GaAs heterostructures with low-temperature mobility μ as high as 35×10^6 cm^2/Vs[1–3]. Ultra-high quality two-dimensional electron gases (2DEGs) provide a platform to study the most fragile fractional quantum Hall states (FQHSs) in the $N = 1$ Landau level (LL), including the putative non-Abelian $\nu = \frac{5}{2}$ and $\nu = \frac{12}{5}$ FQHS. The existence of $\nu = \frac{5}{2}$ and $\nu = \frac{12}{5}$ states presents fundamental challenges to our understanding of correlations in the fractional quantum Hall regime and may provide a platform for exploration of exotic braiding statistics[4]. However, it is often difficult to assess the quality of a given sample by measurement of mobility alone[2,3,5–8]. It has been proposed that the quantum scattering time (or quantum lifetime), $\tau_{\rm q}$, may be a better predictor of the strength of FQHSs at low temperatures and can be used to quantify disorder-induced Landau level broadening[5]. In this study, we investigate the relationship between $\tau_{\rm q}$, 2DEG density variations, and the strength of $\nu = \frac{5}{2}$ FQHS in the ultra-high quality GaAs quantum wells. Our main findings can be summarized as follows: 1) in 2DEGs with sufficiently large $\tau_{\rm q}$, small density inhomogeneities result in non-linear Dingle plots and underestimate $\tau_{\rm q}$ unless density inhomogeneity is explicitly considered; 2) we have developed a method to determine density inhomogeneity from Shubnikov-de Haas (SdH) oscillations and extract the intrinsic $\tau_{\rm q}$; 3) $\tau_{\rm q}$ does not correlate with sample quality as measured by $\Delta_{5/2}$, the excitation gap at 5/2 filling.

II. DEFINITION OF LIFETIMES

Mobility can be recast as a transport lifetime, $\tau_{\rm t} = m^*\mu/e$, that depends on the electron effective mass, m^*, the mobility, μ, and the electronic charge, e. $\tau_{\rm t}$ is particularly sensitive to large-angle scattering. This can be seen in its defining integral[9]

$$\frac{1}{\tau_{\rm t}} = \frac{m^*}{\pi\hbar^3}\int_0^\pi |V_{\boldsymbol{q}}|^2(1-\cos\theta)\,{\rm d}\theta \tag{1}$$

with $|V_{\boldsymbol{q}}|$ being the probability of scattering through an angle θ from a state $\boldsymbol{k}$ to a state $\boldsymbol{k}'$ on the Fermi surface. Note $q = 2k_{\rm F}\sin(\frac{\theta}{2})$ and the Fermi wave-vector $k_{\rm F} = \sqrt{2\pi n}$, n is the 2DEG density. The factor of $(1-\cos\theta)$ in the integral results in reduced weighting of small-angle scattering. Historically, mobility has been the primary metric of 2DEG quality.

The quantum lifetime is another measure of 2DEG quality that is often used in conjunction with mobility measurements to determine dominant scattering mechanisms[9–12]. Unlike $\tau_{\rm t}$, the quantum lifetime weights all scattering events equally. The quantum lifetime is defined as[9]:

$$\frac{1}{\tau_{\rm q}} = \frac{m^*}{\pi\hbar^3}\int_0^\pi |V_{\boldsymbol{q}}|^2\,{\rm d}\theta \tag{2}$$

It measures the mean time a carrier remains in a particular momentum eigenstate before being scattered into a different state. Extraction of $\tau_{\rm q}$ is usually accomplished with transport measurements through analysis of low magnetic field Shubnikov-de Haas oscillations.

The density of states $g(\epsilon)$ of a 2DEG becomes oscillatory at low magnetic field[13–15]. The functional form of $\Delta g(\epsilon)/g_0$ was derived by Isihara and Smrcka[16]

$$\frac{\Delta g}{g_0} = 2\sum_{s=1}^{\infty}\exp(-\frac{\pi s}{\omega_{\rm c}\tau_{\rm q}})\cos(\frac{2\pi\epsilon s}{\hbar\omega_{\rm c}} - s\pi) \tag{3}$$

where $\omega_{\rm c} = eB/m^*$ is the cyclotron frequency, ϵ is the electron energy, and g_0 is the 2D density of states at zero magnetic field. Here the quantum lifetime is related to the width of disorder-broadened Landau levels (Γ) through the relationship $\tau_{\rm q} = \hbar/2\Gamma$. The broadening of the Landau levels is also assumed to be Lorentzian and independent of energy and magnetic field. At small magnetic fields, $\omega_{\rm c}\tau_{\rm q} \sim 1$; retaining only the $s = 1$ term in the density of states, the functional form for SdH oscillations can be written as:

$$\Delta R_{xx} = 4R_o\exp(\frac{-\pi}{\omega_{\rm c}\tau_{\rm q}})\cos(\frac{2\hbar\pi^2 n}{m^*\omega_{\rm c}} - \pi)\chi(T) \tag{4}$$

where R_o is the zero field resistance, and $\chi(T)$, a thermal damping factor, is given by $\chi(T) = (2\pi^2 k_{\rm B}T/\hbar\omega_{\rm c})/\sinh(2\pi^2 k_{\rm B}T/\hbar\omega_{\rm c})$.

In a formalism codified by Coleridge *et al.*[17,18] $\tau_{\rm q}$ can be related to the amplitude of developing Shubnikov-de Haas oscillations by the expression:

$$\Delta R = 4R_o\chi(T)\exp(-\pi/\omega_{\rm c}\tau_{\rm q}) \tag{5}$$

Thus $1/\tau_{\rm q}$ can be extracted directly from the slope of $\Delta R/(4R_o\chi(T))$ plotted versus $1/B$ in natural logarithm scale, also known as a Dingle plot. Assuming a homogeneous 2DEG, data plotted in this manner should fall on a straight line with a $1/B = 0$ intercept of 4. As discussed below, this assumption is often far from valid for the highest quality 2DEGs available today, requiring a more sophisticated application of the Dingle plot formalism in order to extract $1/\tau_{\rm q}$.

III. SAMPLE DESIGN AND EXPERIMENTAL DETAILS

We present measurements on *in situ* back-gated 2DEGs grown by MBE. The 2DEG resides in a 30 nm GaAs quantum well bounded by $Al_{0.24}Ga_{0.76}As$ barriers. Charge transfer to the quantum well is accomplished by δ-doping silicon in narrow GaAs layers flanked by pure AlAs layers placed 66 nm above the principal 30 nm GaAs quantum well. This design has been shown to yield the largest gap energy for the $\nu = \frac{5}{2}$ FQHS[2,19–22]. The *in situ* gate is an n^+ GaAs layer situated 850 nm below the bottom interface of the quantum well. Leakage from gate to 2DEG is minimized by a 830 nm GaAs/AlAs superlattice in the intervening layer. The exact heterostrcture design and processing details can be found in Ref.[20]. The 2DEG density can typically be tuned from depletion to $4 \times 10^{11}/\mathrm{cm}^2$ without significant gate leakage (for larger gate voltages, leakage current exceeds 10 pA which causes excessive electron heating). We have measured three devices on the same chip, sharing a global back gate. Each device is a 1 mm $\times$ 1 mm lithographically-defined van der Pauw square with eight contacts on the edges. Most of the data was taken after briefly illuminating the samples with a red LED, although one exception to this is noted in the text. This particular wafer was chosen because it exhibits the largest $\Delta_{5/2} = 0.625$ K reported to date. We performed standard low frequency lock-in measurments. Typically, for these low-field measurements, the excitation current $I = 200$ nA at $T = 0.3$ K and $I = 50$ nA at $T = 0.01$ K.

IV. EXTRACTION OF $\tau_\mathbf{q}$: IMPACT OF DENSITY INHOMOGENEITY

Fig. 1a shows the magnetoresistance of a device at zero gate bias after subtraction of a smooth background (mean magnetoresistance at each field). The resistance is measured by monitoring the voltage drop along one edge of the sample while driving current between two contacts at the center of opposing faces of the square. The amplitude of the oscillations appears to be described by a single envelope function and no beating is observed. The density spectrum obtained from a fast Fourier transform (FFT) of ΔR_{xx} vs. $1/B$ is shown in Fig. 1b. Only a narrow fundamental peak associated with the nominal 2DEG density and exact higher-order harmonics are observed[23], indicating the sample does not suffer from gross density inhomogeneity or from two or more regions with distinct densities[24]. As we demonstrate below, however, it is likely that small density inhomogeneities in these samples

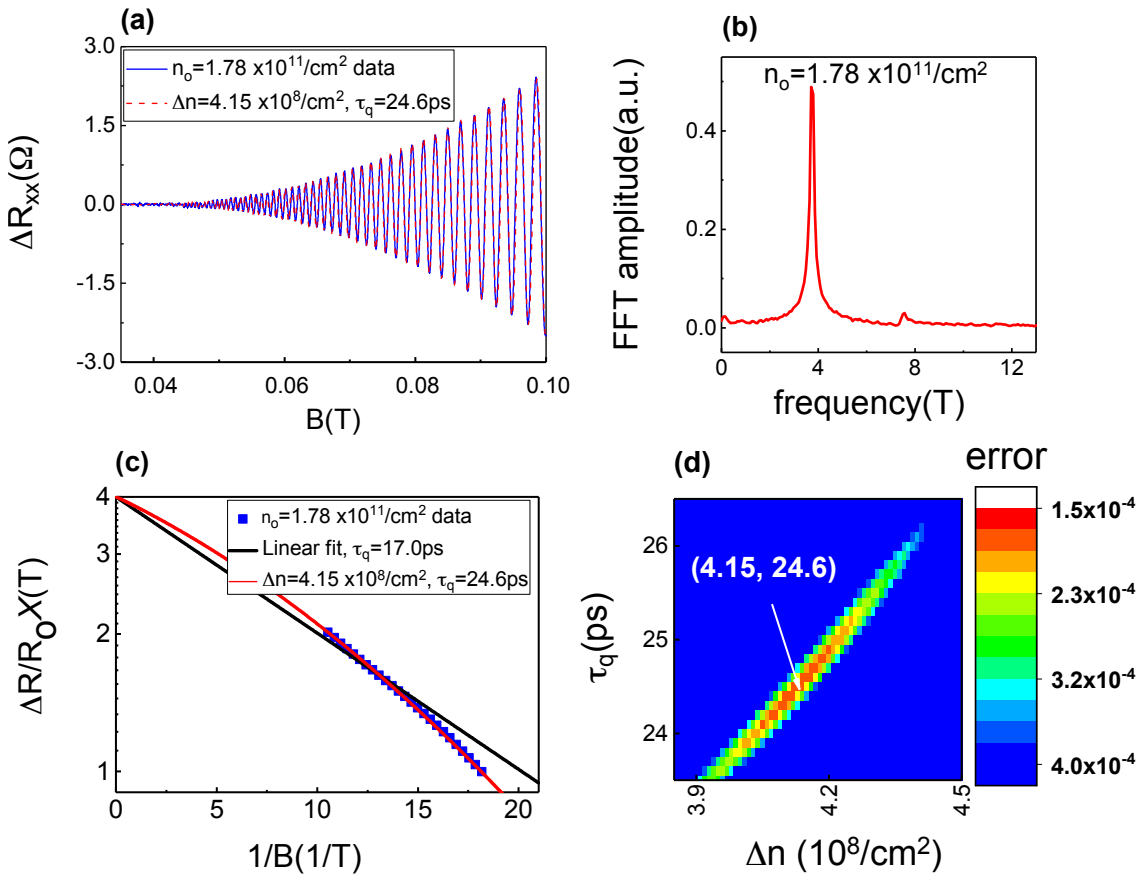

FIG. 1. (color online). Impact of density inhomogeneity on low field transport measured at $T = 0.3$ K. (a) Magnetoresistance as a function of B after background subtraction for nominal 2DEG density $n_o = 1.78 \times 10^{11}/\mathrm{cm}^2$ and simulated trace with $\Delta n/n_o \sim 0.23$ % density inhomogeneity and $\tau_q = 24.6$ ps (red). (b) Density spectrum obtained through a FFT of ΔR_{xx} vs $1/B$. (c) Dingle plots from data (blue squares) and simulated trace (red line) shown in (a). The black line is a single-parameter least square fit of the data between 55 mT and 95 mT with intercept fixed to 4; it clearly shows poor overlap with the data. (d) Two-dimensional plot of the fit error for various combinations of Δn and τ_{q} for data shown in (a). The fit error is minimized at $\Delta n = 4.15 \times 10^8$ cm^{-2} and $\tau_{\mathrm{q}} = 24.6$ ps.

limit the onset of SdH oscillations at low magnetic field[25].

Fig. 1c is a Dingle plot for the data in Fig. 1a. A single-parameter least square fit of the data between 55 mT and 95 mT yields a quantum lifetime $\tau_{\mathrm{q}} = 17$ ps. However, the data points clearly deviate from the straight line expected for a sample with homogeneous

density[18].

It is known that even slight density inhomogeneities or gradients can impact transport at high magnetic fields in the quantum Hall regime[26–31]. For example Pan and collaborators[28] demonstrated that a 1%/cm density gradient in high quality AlGaAs/GaAs 2DEGs could explain quantization of diagonal resistance in the $N = 1$ LL at $T \sim 9$ mK. The sample geometry explored in Ref.[28] is similar to that employed for our experiments. As we show below, minute levels of inhomogeneity can also dominate the low field magnetoresistance when small angle scattering has been strongly suppressed by strong screening of remote scattering centers. For the data shown in Fig. 1a, the onset of SdH oscillations is around 45 mT at $T = 0.3$ K, corresponding to filling factor $\nu \sim 165$, where $\nu = nh/eB$ (in SI units). At a qualitative level, this onset field could correspond to Landau level broadening associated with $\tau_{\rm q}$. On the other hand, density inhomogeneity on the order of $1/\nu \sim 1/165 \sim 0.6\%$ will preclude observation of well-defined oscillations at lower magnetic field even in the limit of infinite $\tau_{\rm q}$.

In order to model the effect of inhomogeneities quantitatively, we assume a Gaussian distribution of densities n_i around nominal density n_o with standard deviation Δn. The 2DEG density distribution is then described by

$$g(n_i) = \frac{1}{\Delta n\sqrt{2\pi}} e^{-\frac{1}{2}(\frac{n_i - n_o}{\Delta n})^2} \tag{6}$$

where n_o is the nominal 2DEG density obtained from FFT spectrum of ΔR_{xx} vs. 1/B. For computational purposes the densities are discretized and evenly spaced, and the weight given to each discrete density n_i is denoted as $P(n_i)$. The densities are discretized and evenly spaced by $\Delta d = 6\Delta n/(2M + 1)$, where M is the number of discrete density values included in the calculation (typically 100 in our simulations). The weight of density n_i is given by

$$P(n_i) = \int_{n_i - \Delta d/2}^{n_i + \Delta d/2} g(n_i) dn_i \tag{7}$$

which can be evaluated as

$$P(n_i) = \frac{1}{2}[\mathrm{erf}(\frac{-n_i + \Delta d/2 + n_o}{\sqrt{2}\Delta n}) - \mathrm{erf}(\frac{-n_i - \Delta d/2 + n_o}{\sqrt{2}\Delta n})] \tag{8}$$

where erf(x) is the error function defined as

$$\mathrm{erf}(x) = \frac{2}{\sqrt{\pi}} \int_0^x e^{-t^2} dt \tag{9}$$

It is assumed that each density carries the same quantum lifetime τ_q. The resultant magnetotransport at low field then can be expressed as the sum of the distribution of all partial SdH oscillations

$$\Delta R_{xx} = 4R_o \sum_{i=1}^{m} P(n_i) \exp(\frac{-\pi}{\omega_c \tau_q}) \cos(\frac{2\hbar\pi^2 n_i}{m^* \omega_c} - \pi)\chi(T) \tag{10}$$

This sum of a spread of oscillation frequencies (expressed in $1/B$) damps the net oscilla-

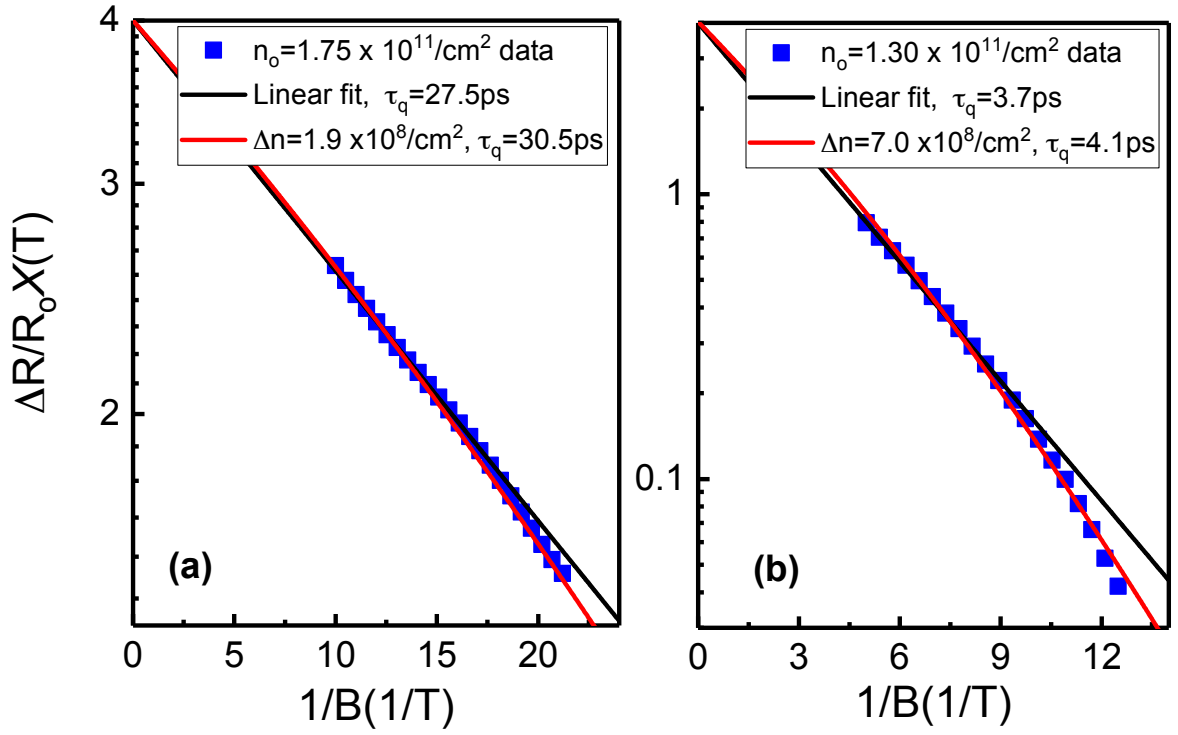

FIG. 2. (color online). Dingle plots from data taken at $T = 0.3$ K and simulations. (a) Back gate 2DEG with nominal 2DEG density $n_o = 1.75 \times 10^{11}/\mathrm{cm}^2$. (b) A 91 nm deep, single heterojunction 2DEG, $n_o = 1.30 \times 10^{11}/\mathrm{cm}^2$.

tion amplitude heavily at small B and results in curvature in a Dingle plot. For samples with low scattering rates (that is, very high quality and long τ_q), the effect can be enormous. Throughout this paper, Dingle plots are superimposed with simulation results after performing error analysis to obtain the best-fit Δn and τ_q. We define the fit error as:

$$\text{error} = \sum_i (\log \Delta R_i^{\text{simulation}} - \log \Delta R_i^{\text{data}})^2 \tag{11}$$

In this expression, i represents each discrete point in the Dingle plot (such as the data points shown in Fig.1 (c)). These points are evenly spaced in terms of $1/B$. We define the error in terms of the logarithm of the oscillation amplitude in order to account for the exponential factor in Eq. 5; this ensures that the the high-field and low-field data points are weighted equally. We note that this formulation is somewhat different from a typical standard least-square error, which would be defined as:

$$\text{error} = \sum_i (\Delta R_i^{\text{simulation}} - \Delta R_i^{\text{data}})^2 \tag{12}$$

Eq. 12 gives significantly more weight to the high-field data where the amplitude is much larger. This artefact makes Eq. 11 more suitable for obtaining a good fit to the SdH data in the present case.

In Fig. 1d we plot the error calculated from Eq. 11 incurred for various combinations of Δn and τ_{q}, for the data in Fig. 1a. The error is minimized at $\Delta n = 4.15 \times 10^8/\text{cm}^2$ and $\tau_{\text{q}} = 24.6$ ps. Next we compare our data to the simulated SdH oscillations (Fig.1 a) and Dingle plot (Fig.1 c) with a quantum lifetime $\tau_{\text{q}} = 24.6$ ps and density fluctuations $\Delta n/n_o \sim 0.23\%$. The excellent overlap between data and simulation reveals that we are able to determine the level of density inhomogeneity in this sample and reproduce the experimental data. The intrinsic quantum lifetime 24.6 ps obtained after properly accounting for density inhomogeneity is 45% higher than the value of 17 ps obtained from a naive linear fit. Here, the percentage difference is quantified as $(\tau_{\text{intrinsic}} - \tau_{\text{linear fit}})/\tau_{\text{linear fit}}$.

The inaccuracy of τ_{q} extracted from a linear fit to the Dingle plot is exacerbated at larger τ_{q} and lower temperature. Data in Fig. 2a is from the back-gated device (the same chip as discussed in Fig. 1), while data shown in Fig. 2b is from a 2DEG utilizing a different heterostructure known to have shorter τ_{q}. This lower quality 2DEG is formed at an $Al_{0.36}Ga_{0.64}As$/GaAs single heterojunction (SHJ) located 91nm below the surface with silicon uniformly doped in the $Al_{0.36}Ga_{0.64}As$ layer. The low field data is collected at $T = 0.3$ K. For the single heterojunction wafer in Fig. 2b we find density inhomogeneity $\Delta n/n_o \sim 0.5\%$ and we find that after accounting for the effect of density inhomogeneity, the calculated τ_q increases by 10%. For the back-gated wafer in Fig. 2a we find density inhomogeneity $\Delta n/n_o \sim 0.1\%$ and we find that the calculated τ_{q} also increases by 10% when accounting for density inhomogeneity. This confirms our expectation that higher quality samples are most sensitive to the impact of density inhomogeneity, since the high-

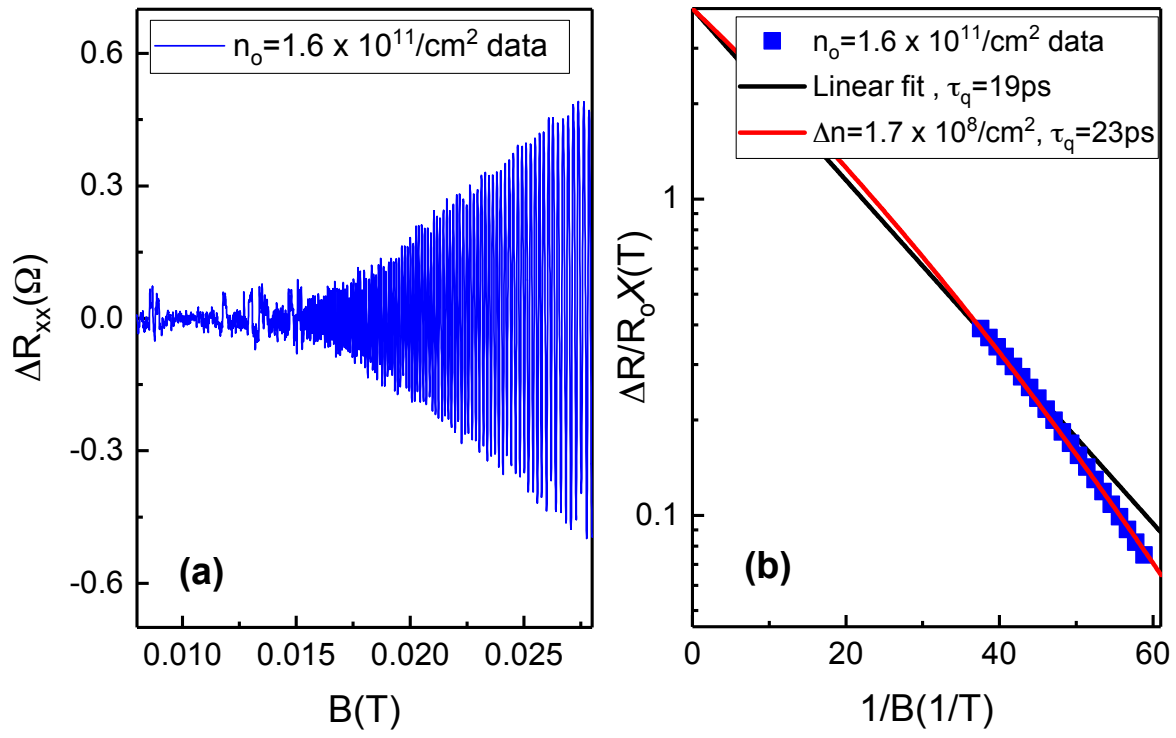

FIG. 3. (color online). Low field transport data of back-gated 2DEG with nominal 2DEG density $n_o = 1.60 \times 10^{11}/\mathrm{cm}^2$ taken at $T = 10$ mK. (a) Magnetoresistance as a function of B after background subtraction. (b) Dingle plots of experimental data and simulation.

quality sample has five times smaller percent density inhomogeneity than the lower-quality SHJ sample, but they both have the same percentage change in τ_{q} after accounting for the effect of density inhomogeneity. This happens because SdH oscillations onset at lower field for higher-quality samples with larger τ_{q}.

The impact of temperature is explored in Fig. 3. Here the back-gated sample is cooled in a dilution refrigerator to reach electron temperature $T = 10$ mK. We have verified that the electron temperature reaches the mixing chamber temperature through careful measurements of the fragile reentrant integer quantum Hall states in the $N = 1$ LL. The thermal damping effect is largely suppressed at this temperature and as a result the SdH oscillation onset moves to lower field (~ 15 mT), as shown in Fig. 3a. Now we compare Fig. 2a and Fig. 3b; data for each plot is from samples with the same heterostructure but measured at different temperatures. They both have $\Delta n/n_o \sim 0.1\%$ density inhomogeneity, but the correction to τ_q is $\sim 20\%$ for the sample measured at $T = 10$ mK compared to 10% at T

= 0.3 K; also, the curvature of the Dingle plot is more visible in the lower temperature data. Both larger τ_q and lower measurement temperature move the onset of SdH oscillation to lower field, or equivalently higher filling factor ν, where density inhomogeneity will have more impact.

V. DENSITY DEPENDENCE OF $\tau_{\mathbf{q}}$ AND $\Delta_{5/2}$

A. scattering dominating $\tau_{\mathbf{q}}$

We extract $\tau_{\rm q}$ from one of the back-gated samples at various densities after accounting for the effect of density inhomogeneity; the results are displayed in Fig. 4. We observe that the quantum lifetime initally increases monotonically from near depletion to $n \sim 1\times 10^{11}/\mathrm{cm}^2$, but it remains nearly constant at around 25ps from $n \sim 1\times 10^{11}/\mathrm{cm}^2$ to $n \sim 2.0\times 10^{11}/\mathrm{cm}^2$ and starts to decrease slightly when density is higher than $2.0\times 10^{11}/\mathrm{cm}^2$. A similar trend was observed in Ref.[7]. The decrease in $\tau_{\rm q}$ at high density is somewhat surprising since, assuming that the distribution of impurities remains the same, $\tau_{\rm q}$ would be expected to increase monotonically with density in a gated device due to the increase of the Fermi wavevector $k_{\rm F}$, as calculated in Ref.[5]. This can be resolved by noting that, in our device, the gate consists of a heavily silicon-doped GaAs layer, and when the density is increased by applying increased positive bias to the gate, an equal number of positively-charged impurities are ionized on the gate to maintain charge neutrality. These ionized donors act as scattering sites, and since their concentration increases linearly with density, $\tau_{\rm q}$ starts to decrease at high densities. At low density, on the other hand, scattering is dominated by fixed charged impurities in the doping well, and $\tau_{\rm q}$ increases monotonically in that range.

In order to quantify this non-monotonic behavior, we performed numerical calculations of $\tau_{\rm q}$ following the approach of Ref.[5,32]. To model the device, we assume that when positive bias is applied to the back gate, the number of ionized impurity scattering sites is equal to the charge transferred from the gate to the 2DEG. When zero or negative bias is applied to the back gate, we assume no impurity scattering is caused by the gate, since all of the donors remain unionized. The impurity concentration on the gate is then

$$n_{\rm gate} = n - n_{V_{\rm G}=0}(n \geq n_{V_{\rm G}=0}) \tag{13}$$

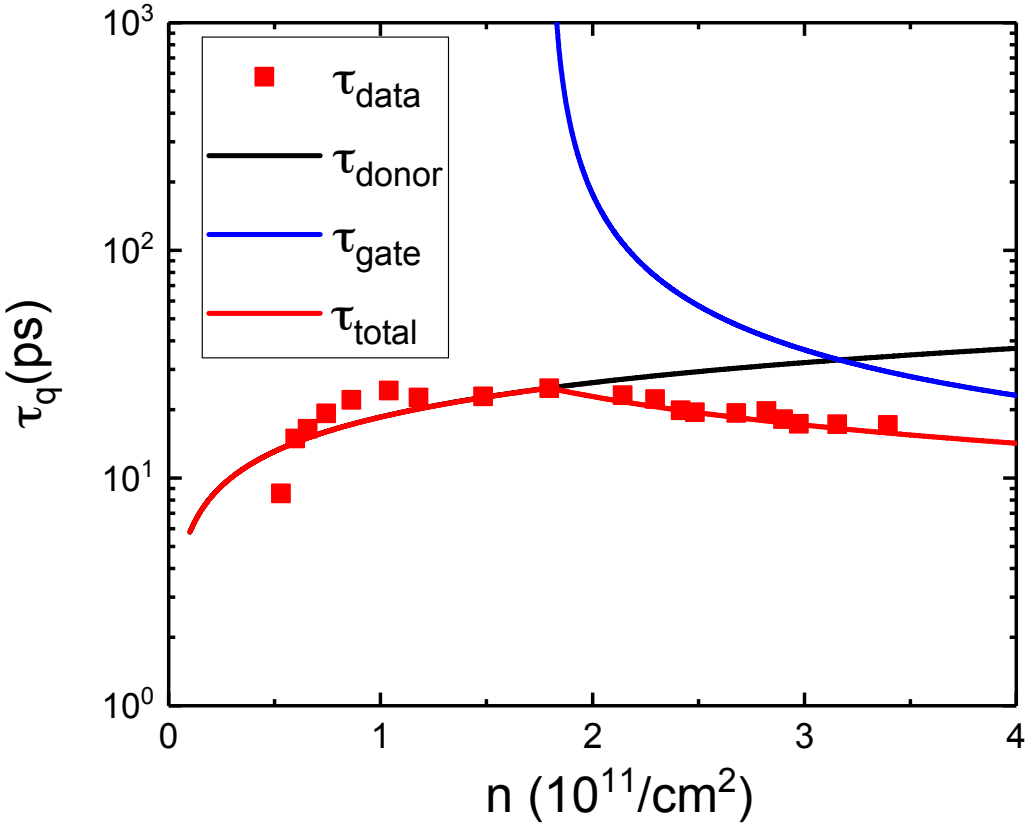

FIG. 4. (color online). Experimentally measured $\tau_{\rm q}$ (red squares) and numerically calculated $\tau_{\rm q}$ (solid lines) as as a function of 2DEG density n. The black line shows the scattering time corresponding to scattering by donors in the doping well, while the black line shows the scattering time corresponding to scattering by ionized impurities on the back gate. The red line shows the combined $\tau_{\rm q}$ including both sources of scattering, and shows reasonable agreement with the experimental data.

and

$$n_{\rm gate} = 0 (n \leq n_{\rm V_G=0}) \tag{14}$$

In these expressions, $n_{\rm gate}$ is the impurity concentration on the back gate and $n_{V_{\rm G}=0}$ is the 2DEG density with zero applied gate bias. An additional complication is that while at $n_{V_{\rm G}=0}$ scattering is expected to be dominated by ionized donors in the doping well, the ionized donors in the doping well are screened by electrons transferred to the X-band of the AlAs barriers surrounding the doping well[2], which reduces the scattering rate by these

donors. To account for this, we extract an effective doping well impurity concentration, $n_{\rm donor}$, by matching the $n_{V_{\rm G}=0}$ quantum lifetime; this gives $n_{\rm donor} = 1.35 \times 10^{10}/{\rm cm}^2$. This is smaller than the actual number of ionized donors, which is $\sim 7 \times 10^{11}/{\rm cm}^2$; evidently screening in the AlAs barriers is highly effective at reducing scattering[2,19–22].

The results of the simulation using these assumptions are presented as solid lines in Fig. 4. We have divided the impurity scattering into the scattering by ionized donors in the doping well (characterized by scattering time $\tau_{\rm donor}$) and scattering by the back gate (characterized by scattering time $\tau_{\rm gate}$). As expected, $\tau_{\rm donor}$ increases as the 2DEG density n increases, while $\tau_{\rm gate}$ decreases when positive bias is applied to the gate and impurities on the gate are ionized. The total quantum lifetime $\tau_{\rm total}$, which takes into account both scattering by the impurities on the gate and in the doping well, shows reasonable agreement with the experimental data, especially when $n > 1.0 \times 10^{11}/{\rm cm}^2$. At lower densities, the calculated $\tau_{\rm total}$ deviates from experimental data; this suggests that at very low densities, the two-impurity model is insufficient. Nevertheless, this simple treatment accounts for the striking experimental result that $\tau_{\rm q}$ decreases as density increases in the high density range.

Most of the data we show is taken after the sample is illuminated with a red LED; this procedure is known to improve sample quality in terms of the strength of the FQHSs[6]. However, in Fig. 5a we also show two representative data points taken with no illumination of the sample. $\tau_{\rm q}$ is lower without illumination, indicating that illumination improves screening of remote impurities that determine $\tau_{\rm q}$. This effect is interesting as the change in $\tau_{\rm q}$ does not accompany an increase in 2DEG density. The illumination and subsequent relaxation simply allows the system to equilibrate to a configuration in which scattering is reduced.

B. comparison between $\tau_{\rm q}$ and $\Delta_{5/2}$

Having acccounted for the impact of density inhomogeneity on $\tau_{\rm q}$ we turn now to the relationship between $\tau_{\rm q}$ and $\Delta_{5/2}^{\rm meas}$, where $\Delta_{5/2}^{\rm meas}$ is the experimentally measured gap, and discuss if $\tau_{\rm q}$ can be used as a metric of quality relevant to $N = 1$ LL. As seen in Fig. 5c, $\Delta_{5/2}^{\rm meas}$ increases nearly monotonically with density. Clearly $\Delta_{5/2}^{\rm meas}$ and $\tau_{\rm q}$ behave differently as a function of density; a concomitant increase in $\tau_{\rm q}$ is not observed in the density regime above $n = 1 \times 10^{11}$ cm^{-2}. We note that our observation that $\Delta_{5/2}^{\rm meas}$ increases with density while $\tau_{\rm q}$ decreases is in direct contradiction with the expectations of Ref.[5]. The simplest

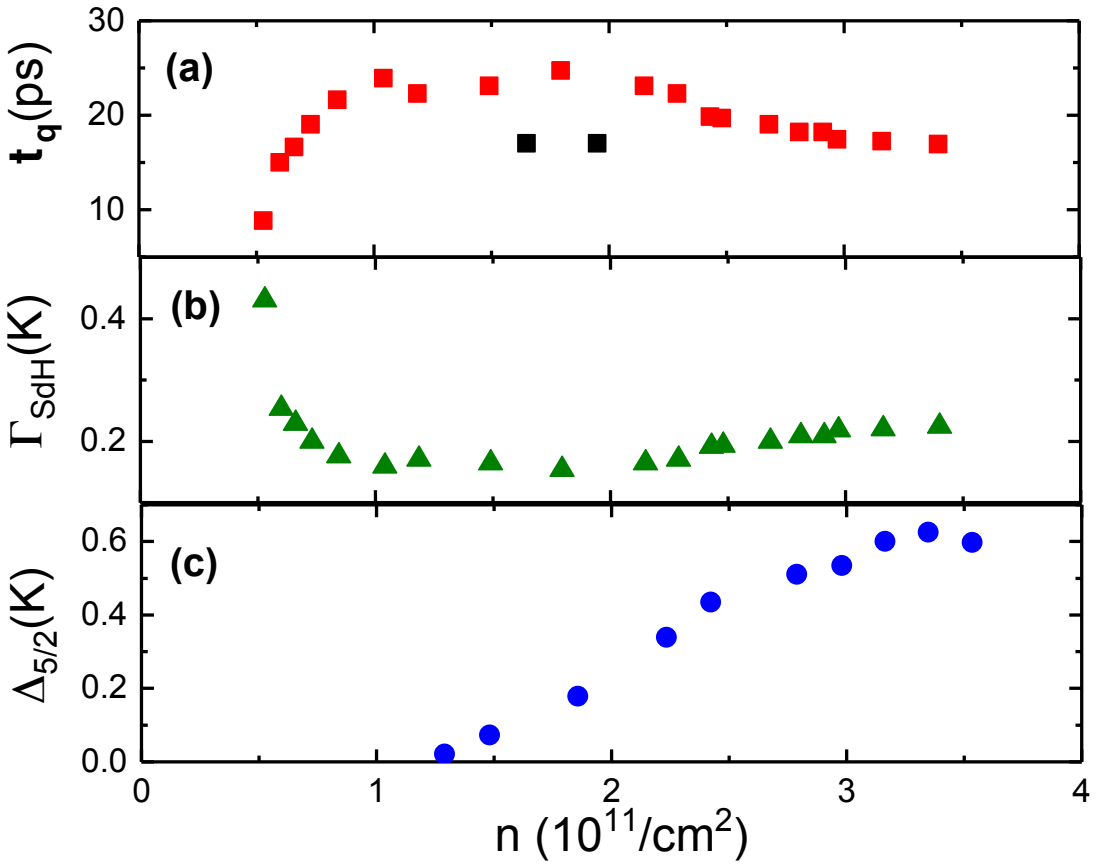

FIG. 5. (color online). Characteristic properties of the back-gated sample as a function of the electron density n. (a) Quantum lifetime $\tau_{\rm q}$ extracted from Shubnikov de-Hass oscillations measured at $T = 0.3$ K, both in dark (black) and after illumination (red). (b) The Landau level broadening based on low-field quantum lifetime time with illumination, $\Gamma_{\rm SdH} = \hbar/2\tau_q$. (c) Gap energy for the $\nu = \frac{5}{2}$ FQHS with illumination.

explanation for this is that the explicit increase of the intrinsic gap with density leads to the increase of the experimentally measured gap, and the effect of decreasing $\tau_{\rm q}$ is overwhelmed. However, it is also possible that $\tau_{\rm q}$ is simply not sensitive to the disorder relevant to $\Delta_{5/2}^{\rm meas}$; in either case, $\tau_{\rm q}$ cannot be used in a simple manner to predict $\Delta_{5/2}^{\rm meas}$ without additional analysis in density-tunable devices.

We convert quantum lifetime to the Landau level broadening using $\Gamma_{\rm SdH} = \hbar/2\tau_q$ as shown in Fig. 5b. $\Gamma_{\rm SdH}$ is usually interpreted as the magnetic field-independent energy broadening of the Landau levels. Then one would expect the relationship $\Delta_{5/2}^{\rm theor} - \Delta_{5/2}^{\rm meas} =$

$\Gamma_{5/2} = \Gamma_{\rm SdH}$[33,34], where $\Delta_{5/2}^{\rm theor}$ is the intristic gap in the absence of disorder. $\Delta_{5/2}^{\rm theor}$ in this density range was numerically calculated in Ref.[7], taking into account the finite width of the quantum well and LL mixing[35]. According to Ref.[7] $\Delta_{5/2}^{\rm theor}$ should exceed 2 K at $n = 3.0\times10^{11}$ cm^{-2}, far above the maximal value of $\Delta_{5/2}^{\rm meas} = 0.625$ K. Clearly $\Gamma_{\rm SdH}$ severely underestimates the level broadening $\Gamma_{5/2}$ relevant to the $\nu = \frac{5}{2}$ state. This observation is consistent with other experiments reported previously[7,36]. However we must be cognizant of the limitations of this analysis. Since the experimentally measured values of $\Delta_{5/2}^{\rm meas}$ are much smaller than the numerically calculated values it follows that small errors in the numerically calculated gap $\Delta_{5/2}^{\rm theor}$ can lead to large changes of $\Gamma_{5/2}$ vs. density, including even its functional density dependence. We also cannot completely rule out the possibility that $\Gamma_{5/2}$ is proportional to $\Gamma_{\rm SdH}$ but differs by a scale factor. Regardless, we are led to the same conclusions as before: $\tau_{\rm q}$ does not correlate directly with the gap $\Delta_{5/2}^{\rm meas}$ nor can the disorder broadening of the $\nu = \frac{5}{2}$ state be simply calculated from the expression $\Gamma = \hbar/2\tau_q$. In Ref.[37], we describe the utility of a different metric of 2DEG quality at $T = 0.3$ K, $\rho_{5/2}$, the high temperature resistivity at $\nu = \frac{5}{2}$ where the state is best described as a Fermi sea of composite fermions. $\rho_{5/2}$ does show correlation with $\Delta_{5/2}$.

VI. CONCLUSIONS

In conclusion, we consistently find that small density inhomogeneities in samples whose scattering from remote ionized impurities has been minimized yield Dingle plots that are non-linear and underestimate $\tau_{\rm q}$. This effect becomes significant with larger τ_q and lower temperature, as both move the onset of SdH oscillations to lower magnetic field where small density fluctuations have a larger impact. We have developed a method to determine this small density inhomogeneity by assuming a Gaussian distribution of 2DEG density and extract the intrinsic quantum lifetime using this method. We observe no correlation between $\tau_{\rm q}$ and $\Delta_{5/2}$ in our density tunable devices, and conclude that $\tau_{\rm q}$ is not useful for predicting the strength of the $\nu = \frac{5}{2}$ FQHS.

VII. ACKNOWLEDGEMENT

This work was supported by the U.S. DOE Office of Basic Energy Sciences, Division of Materials Sciences and Engineering Award No. DE-SC0006671. Additional support for sample growth from the W. M. Keck Foundation and Microsoft Station Q is gratefully acknowledged. SL and JF were supported by the Canada First Research Excellence Fund, QMI, and NSERC.

---

* mmanfra@purdue.edu

[1] Geoffrey C. Gardner, Saeed Fallahi, John D. Watson, Michael J. Manfra, J. Cryst. Growth **441** 71 (2016)

[2] M. J. Manfra, Annu. Rev. Condens. Matter Phys. **5** 347 (2014)

[3] V. Umansky, M. Heiblum, Y. Levinson, J. Smet, J. Nubler, and M. Dolev, J. Cryst. Growth **311** 1658 (2009)

[4] C. Nayak et al., Rev. Mod. Phys. **80**, 1083 (2008)

[5] S. Das Sarma and E. H. Hwang, Phys. Rev. B **90**, 035425 (2014)

[6] G. Gamez and K. Muraki, Phys. Rev. B **88**, 075308 (2013)

[7] J. Nuebler, V. Umansky, R. Morf, M. Heiblum, K. von Klitzing, and J. Smet, Phys. Rev. B **81**, 035316 (2010)

[8] W. Pan, N. Masuhara, N. S. Sullivan, K. W. Baldwin, K. W. West, L. N. Pfeiffer, and D. C. Tsui, Phys. Rev. Lett. **106**, 206806 (2011)

[9] S. Das Sarma and F. Stern, Phys. Rev. B **32**, 8442(R) (1985)

[10] D. Q. Wang, J. C. H. Chen, O. Klochan, K. Das Gupta, D. Reuter, A. D. Wieck, D. A. Ritchie, and A. R. Hamilton, Phys. Rev. B **87**, 195313 (2013)

[11] M. J. Manfra, S. H. Simon, K. W. Baldwin, A. M. Sergent, K. W. West, R. J. Molnar and J. Caissie, Appl. Phys. Lett. **85**, 5278 (2004)

[12] S. J. MacLeod, K. Chan, T. P. Martin, A. R. Hamilton, A. See, A. P. Micolich, M. Aagesen, and P. E. Lindelof, Phys. Rev. B **80**, 035310 (2009)

[13] I. M. Lifshitz and A.M. Kosevich, J. Exper. Theoret. Phys. USSR **29**, 730 (1955)

[14] T. Ando, J. Phys. Soc. Jpn. **37** 1233 (1974)

[15] T. Ando, A. B. Fowler, and F. Stern, Rev. Mod. Phys. **54**, 437 (1982)

[16] A. Isihara and L. Smrcka, J. Phys. C: Solid State Phys. **19**, 6777 (1986)

[17] P. T. Coleridge, R. Stoner, and R. Fletcher, Phys. Rev. B **39**, 1120 (1989)

[18] P. T. Coleridge, Phys. Rev. B **44**, 3793 (1991)

[19] M. Samani, A. V. Rossokhaty, E. Sajadi, S. Luscher, J. A. Folk, J. D. Watson, G. C. Gardner, and M. J. Manfra, Phys. Rev. B **90**, 121405(R) (2014)

[20] J. D. Watson, G. A. Csathy, and M. J. Manfra, Phys. Rev. Appl. **3**, 064004 (2015)

[21] N. Deng, G. C. Gardner, S. Mondal, E. Kleinbaum, M. J. Manfra and G. A. Csathy, Phys. Rev. Lett. **112**, 116804 (2014)

[22] NP Deng, J. D. Watson, L. P. Rokhinson, M. J. Manfra, and G. A. Csathy, Phys. Rev. B **86**, 201301 (2012)

[23] A. Endo, and Y. Iye, Journ. Phys. Soc. Japan **77**, 064713 (2008)

[24] W. Zhou, H. M. Yoo, S. Prabhu-Gaunkar, L. Tiemann, C. Reichl, W. Wegscheider, M. Grayson, Phys. Rev. Lett. **115**, 186804 (2015)

[25] S. Syed, M. J. Manfra, Y. J. Wang, R. J. Molnar, and H. L. Stormer, Appl. Phys. Lett. **84**, 1507 (2004)

[26] H. L. Stormer, K. W. Baldwin, L. N. Pfeiffer, and K. W. West, Sol. State Comm. **84**, 95 (1992)

[27] S. H. Simon, and B. I. Halperin, Phys. Rev. Lett. **73**, 3278 (1994)

[28] W. Pan, J. S. Xia, H. L. Stormer, D. C. Tsui, C. L. Vicente, E. D. Adams, N. S. Sullivan, L. N. Pfeiffer, K. W. Baldwin, and K. W. West, Phys. Rev. Lett. **95**, 066808 (2005)

[29] R. Ilan, N. R. Cooper, and Ady Stern, Phys. Rev. B **73**, 235333 (2006)

[30] W. Pan et al., Sol. State Comm. **140**, 88 (2006)

[31] T. Khouri et al., Phys. Rev. Lett.**117**, 256601 (2016)

[32] See equations 12-16 in Ref.[5] for theoretical calculation details.

[33] A. M. Chang, M. A. Paalanen, D. C. Tsui, H. L. Stormer, and J. C. M. Hwang, Phys. Rev. B **28**, 6133 (1983)

[34] C. R. Dean, B. A. Piot, P. Hayden, S. Das Sarma, G. Gervais, L. N. Pfeiffer, and K. W. West, Phys. Rev. Lett. **100**, 146803 (2008)

[35] R. Morf and N. dAmbrumenil, Phys. Rev. B **68**, 113309 (2003)

[36] N. Samkharadze, J. D.Watson, G. Gardner, M. J. Manfra, L. N. Pfeiffer, K.W.West, and G. A. Csathy, Phys. Rev. B **84**, 121305(R) (2011)

[37] Q. Qian, J. Nakamura, S. Fallahi, G. C. Gardner, J. D. Watson, and M. J. Manfra, Phys. Rev. B **95**, 241304(R) (2017)